Momentum Contrast for Unsupervised Visual Representation Learning

Kaiming He Haoqi Fan Yuxin Wu Saining Xie Ross Girshick
Facebook AI Research (FAIR)
Code: https://github.com/facebookresearch/moco

Abstract

We present Momentum Contrast (MoCo) for unsuper- vised visual representation learning. From a perspective on contrastive learning [25] as dictionary look-up, we build a dynamic dictionary with a queue and a moving-averaged encoder. This enables building a large and consistent dic- tionary on-the-fly that facilitates contrastive unsupervised learning. MoCo provides competitive results under the common linear protocol on ImageNet classification. More importantly, the representations learned by MoCo transfer well to downstream tasks. MoCo can outperform its super- vised pre-training counterpart in 7 detection/segmentation tasks on PASCAL VOC, COCO, and other datasets, some- times surpassing it by large margins. This suggests that the gap between unsupervised and supervised representa- tion learning has been largely closed in many vision tasks.

1 Introduction

Unsupervised representation learning is highly success- ful in natural language processing, e.g., as shown by GPT [43, 44] and BERT [10]. But supervised pre-training is still dominant in computer vision, where unsupervised meth- ods generally lag behind. The reason may stem from dif- ferences in their respective signal spaces. Language tasks have discrete signal spaces (words, sub-word units, etc.) for building tokenized dictionaries, on which unsupervised learning can be based. Computer vision, in contrast, further concerns dictionary building [46, 7, 4], as the raw signal is in a continuous, high-dimensional space and is not struc- tured for human communication (e.g., unlike words). Several recent studies [52, 49, 31, 56, 30, 48, 1] present promising results on unsupervised visual representation learning using approaches related to the contrastive loss [25]. Though driven by various motivations, these methods can be thought of as building dynamic dictionaries. The "keys" (tokens) in the dictionary are sampled from data (e.g., images or patches) and are represented by an encoder network. Unsupervised learning trains encoders to perform dictionary look-up: an encoded "query" should be similar to its matching key and dissimilar to others. Learning is formulated as minimizing a contrastive loss [25].

From this perspective, we hypothesize that it is desirable to build dictionaries that are: (i) large and (ii) consistent as they evolve during training. Intuitively, a larger dictio- nary may better sample the underlying continuous, high- dimensional visual space, while the keys in the dictionary should be represented by the same or similar encoder so that their comparisons to the query are consistent. However, ex- isting methods that use contrastive losses can be limited in one of these two aspects (discussed later in context). We present Momentum Contrast (MoCo) as a way of building large and consistent dictionaries for unsupervised learning with a contrastive loss (Figure 1). We maintain the dictionary as a queue of data samples: the encoded repre- sentations of the current mini-batch are enqueued, and the oldest are dequeued. The queue decouples the dictionary size from the mini-batch size, allowing it to be large. Moreover, as the dictionary keys come from the preceding sev- eral mini-batches, a slowly progressing key encoder, imple- mented as a momentum-based moving average of the query encoder, is proposed to maintain consistency. MoCo is a mechanism for building dynamic dictionar- ies for contrastive learning, and can be used with various pretext tasks. In this paper, we follow a simple instance discrimination task [52? , 1]: a query matches a key if they are encoded views (e.g., different crops) of the same image. Using this pretext task, MoCo shows competitive results under the common protocol of linear classification in the ImageNet dataset [9]. A main purpose of unsupervised learning is to pre-train representations (i.e., features) that can be transferred to downstream tasks by fine-tuning. We show that in 7 down- stream tasks related to detection or segmentation, MoCo unsupervised pre-training can surpass its ImageNet super- vised counterpart, in some cases by nontrivial margins. In these experiments, we explore MoCo pre-trained on ImageNet or on a one-billion Instagram image set, demonstrat- ing that MoCo can work well in a more real-world, billion- image scale, and relatively uncurated scenario. These re- sults show that MoCo largely closes the gap between un- supervised and supervised representation learning in many computer vision tasks, and can serve as an alternative to Im- ageNet supervised pre-training in several applications.

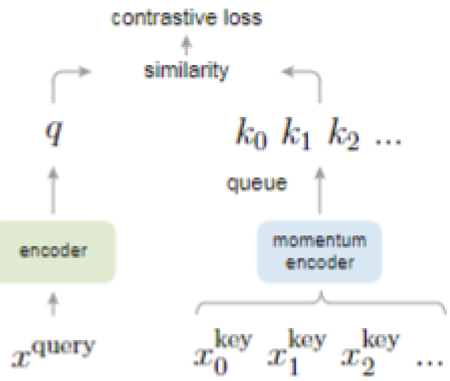

Figure 1: Momentum Contrast (MoCo) trains a visual representation encoder by matching an encoded query q to a dictionary of encoded keys using a contrastive loss. The dictionary keys k0, k1, k2, ... are defined on-the-fly by a set of data samples. The dictionary is built as a queue, with the current mini-batch en- queued and the oldest mini-batch dequeued, decoupling it from the mini-batch size. The keys are encoded by a slowly progressing encoder, driven by a momentum update with the query encoder. This method enables a large and consistent dictionary for learning visual representations.

2 Related Work

Unsupervised/self-supervised1 learning methods gener- ally involve two aspects: pretext tasks and loss functions. The term "pretext" implies that the task being solved is not of genuine interest, but is solved only for the true purpose of learning a good data representation. Loss functions can often be investigated independently of pretext tasks. MoCo focuses on the loss function aspect. Next we discuss related studies with respect to these two aspects. Loss functions. A common way of defining a loss function is to measure the difference between a model's prediction and a fixed target, such as reconstructing the input pixels (e.g., auto-encoders) by L1 or L2 losses, or classifying the input into pre-defined categories (e.g., eight positions [11], color bins [55]) by cross-entropy or margin-based losses. Other alternatives, as described next, are also possible. Contrastive losses [25] measure the similarities of sample pairs in a representation space. Instead of matching an input to a fixed target, in contrastive loss formulations the target can vary on-the-fly during training and can be defined in terms of the data representation computed by a network [25]. Contrastive learning is at the core of several recent works on unsupervised learning [52, 49, 31, 56, 30, 48, 1], which we elaborate on later in context (Sec. 3.1). Adversarial losses [19] measure the difference between probability distributions. It is a widely successful technique for unsupervised data generation. Adversarial methods for representation learning are explored in [**?** **?**]. There are relations (see [19]) between generative adversarial networks and noise-contrastive estimation (NCE) [24]. Pretext tasks. A wide range of pretext tasks have been pro- posed. Examples include recovering the input under some corruption, e.g., denoising auto-encoders [**?**], context auto- encoders [41], or cross-channel auto-encoders (coloriza- tion) [55**?**]. Some pretext tasks form pseudo-labels by, e.g., transformations of a single ("exemplar") image [13], patch orderings [11, 40], tracking [50] or segmenting ob- jects [**?**] in videos, or clustering features [2, 3]. Contrastive learning vs. pretext tasks. Various pretext tasks can be based on some form of contrastive loss func- tions. The instance discrimination method [52] is related to the exemplar-based task [13] and NCE [24]. The pretext task in contrastive predictive coding (CPC) [49] is a form of context auto-encoding [41], and in contrastive multiview coding (CMC) [48] it is related to colorization [55].

3 Method

3.1 Contrastive Learning as Dictionary Look-up

Contrastive learning [25], and its recent developments, can be thought of as training an encoder for a dictionary look-up task, as described next. Consider an encoded query q and a set of encoded sam- ples k0, k1, k2, ... that are the keys of a dictionary. As- sume that there is a single key (denoted as k+) in the dic- tionary that q matches. A contrastive loss [25] is a function whose value is low when q is similar to its positive key k+ and dissimilar to all other keys (considered negative keys for q). With similarity measured by dot product, a form of a contrastive loss function, called InfoNCE [49], is consid- ered in this paper:

$$L(q,k+) = -\log \frac{\exp(q^T k^+)}{\sum_{i=0}^{K} \exp(q^T k_i^+)} \tag{1}$$

where τ is a temperature hyper-parameter per [52]. The sum is over one positive and K negative samples. Intuitively, this loss is the log loss of a (K+1)-way softmax-based clas- sifier that tries to classify q as k+. Contrastive loss functions can also be based on other forms [25, 50, 52, 31], such as margin-based losses and variants of NCE losses. The contrastive loss serves as an unsupervised objective function for training the encoder networks that represent the queries and keys [25]. In general, the query representation is q = fq(xq) where fq is an encoder network and xq is a query sample (likewise, k = fk(xk)). Their instantiations depend on the specific pretext task. The input xq and xk can be images [25, 52**?**], patches [49], or context consisting a set of patches [49]. The networks fq and fk can be identical [25, 50**?**], partially shared [49, 31, 1], or different [48].

3.2 Momentum Contrast

From the above perspective, contrastive learning is a way of building a discrete dictionary on high-dimensional con- tinuous inputs such as images. The dictionary is dynamic in the sense that the keys are randomly sampled, and that the key encoder evolves during training. Our hypothesis is that good features can be learned by a large dictionary that cov- ers a rich set of negative samples, while the encoder for the dictionary keys is kept as consistent as possible despite its evolution. Based on this motivation, we present Momentum Contrast as described next. Dictionary as a queue. At the core of our approach is maintaining the dictionary as a queue of data samples. This allows us to reuse the encoded keys from the immediate preceding mini-batches. The introduction of a queue decouples the dictionary size from the mini-batch size. Our dictionary size can be much larger than a typical mini-batch size, and can be flexibly and independently set as a hyper-parameter. The samples in the dictionary are progressively replaced. The current mini-batch is enqueued to the dictionary, and the oldest mini-batch in the queue is removed. The dictio- nary always represents a sampled subset of all data, while the extra computation of maintaining this dictionary is man- ageable. Moreover, removing the oldest mini-batch can be beneficial, because its encoded keys are the most outdated and thus the least consistent with the newest ones. Momentum update. Using a queue can make the dictio- nary large, but it also makes it intractable to update the key encoder by back-propagation (the gradient should propa- gate to all samples in the queue). A naïve solution is to copy the key encoder fk from the query encoder fq, ignor- ing this gradient. But this solution yields poor results in experiments (Sec. 4.1). We hypothesize that such failure is caused by the rapidly changing encoder that reduces the key representations' consistency. We propose a momentum update to address this issue. Formally, denoting the parameters of f_k as θ_k and those of f_q as θ_q, we update θ_k by:

$$\theta_k = m\theta_k + (1-m)\theta_q \tag{2}$$

Here m ε [0, 1) is a momentum coefficient. Only the parameters θ_q are updated by back-propagation. The momentum update in Eqn.(2) makes θ_k evolve more smoothly than θ_q. As a result, though the keys in the queue are encoded by different encoders (in different mini-batches), the dif- ference among these encoders can be made small. In ex- periments, a relatively large momentum (e.g., m = 0.999, our default) works much better than a smaller value (e.g., m = 0.9), suggesting that a slowly evolving key encoder is a core to making use of a queue. Relations to previous mechanisms. MoCo is a general mechanism for using contrastive losses. We compare it with two existing general mechanisms in Figure 2. They exhibit different properties on the dictionary size and consistency. The end-to-end update by back-propagation is a natural mechanism

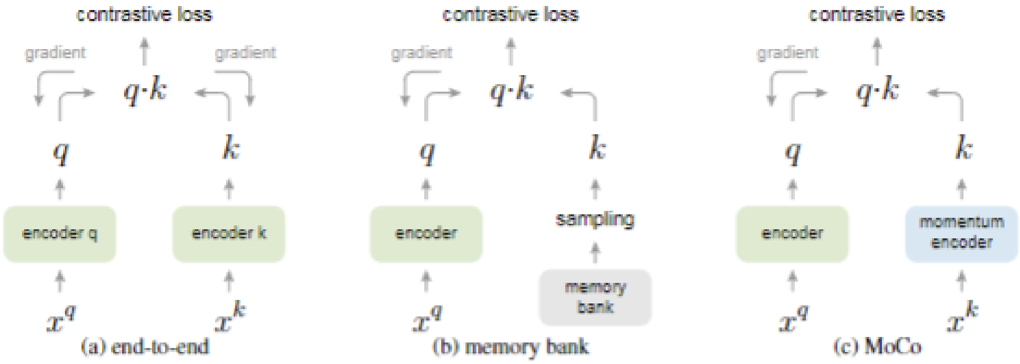

Figure 2: Conceptual comparison of three contrastive loss mechanisms (empirical comparisons are in Figure 3 and Table 3). Here we illustrate one pair of query and key. The three mechanisms differ in how the keys are maintained and how the key encoder is updated. (a): The encoders for computing the query and key representations are updated end-to-end by back-propagation (the two encoders can be different). (b): The key representations are sampled from a memory bank [52]. (c): MoCo encodes the new keys on-the-fly by a momentum-updated encoder, and maintains a queue (not illustrated in this figure) of keys.

(e.g., [25, 49, 31**?** , 1, 30], Figure 2a). It uses samples in the current mini-batch as the dictionary, so the keys are consistently encoded (by the same set of encoder parameters). But the dictionary size is coupled with the mini-batch size, limited by the GPU memory size. It is also challenged by large mini-batch optimization [20]. Some re- cent methods [49, 31, 1] are based on pretext tasks driven by local positions, where the dictionary size can be made larger by multiple positions. But these pretext tasks may require special network designs such as patchifying the input [49] or customizing the receptive field size [1], which may com- plicate the transfer of these networks to downstream tasks. Another mechanism is the memory bank approach proposed by [52] (Figure 2b). A memory bank consists of the representations of all samples in the dataset. The dictionary for each mini-batch is randomly sampled from the memory bank with no back-propagation, so it can support a large dictionary size. However, the representation of a sample in

Algorithm 1 Pseudocode of MoCo in a PyTorch-like style.

```
# f_q, f_k: encoder networks for query and key
# queue: dictionary as a queue of K keys (CxK)
# m: momentum
# t: temperature

f_k.params = f_q.params # initialize
for x in loader: # load a minibatch x with N samples
    x_q = aug(x) # a randomly augmented version
    x_k = aug(x) # another randomly augmented version

    q = f_q.forward(x_q) # queries: NxC
    k = f_k.forward(x_k) # keys: NxC
    k = k.detach() # no gradient to keys

    # positive logits: Nx1
    l_pos = bmm(q.view(N,1,C), k.view(N,C,1))

    # negative logits: NxK
    l_neg = mm(q.view(N,C), queue.view(C,K))

    # logits: Nx(1+K)
    logits = cat([l_pos, l_neg], dim=1)

    # contrastive loss, Eqn.(1)
    labels = zeros(N) # positives are the 0-th
    loss = CrossEntropyLoss(logits/t, labels)

    # SGD update: query network
    loss.backward()
    update(f_q.params)

    # momentum update: key network
    f_k.params = m*f_k.params+(1-m)*f_q.params

    # update dictionary
    enqueue(queue, k) # enqueue the current minibatch
    dequeue(queue) # dequeue the earliest minibatch
```

bmm: batch matrix multiplication; mm: matrix multiplication; cat: concatenation.

the memory bank was updated when it was last seen, so the sampled keys are essentially about the encoders at multiple different steps all over the past epoch and thus are less con- sistent. A momentum update is adopted on the memory bank in [52]. Its momentum update is on the representa- tions of the same sample, not the encoder. This momentum update is irrelevant to our method, because MoCo does not keep track of every sample. Moreover, our method is more memory-efficient and can be trained on billion-scale data, which can be intractable for a memory bank. Sec. 4 empirically compares these three mechanisms.

3.3 Pretext Task

Contrastive learning can drive a variety of pretext tasks. As the focus of this paper is not on designing a new pretext task, we use a simple one mainly following the instance discrimination task in [52], to which some recent works [54, 1] are related. Following [52], we consider a query and a key as a pos- itive pair if they originate from the same image, and other- wise as a negative sample pair. Following [54, 1], we take two random "views" of the same image under random data augmentation to form a positive pair. The queries and keys are respectively encoded by their encoders, f_q and f_k. The encoder can be any convolutional neural network [34]. Algorithm 1 provides the pseudo-code of MoCo for this pretext task. For the current mini-batch, we encode the queries and their corresponding keys, which form the posi- tive sample pairs. The negative samples are from the queue. Technical details. We adopt a ResNet [34] as the encoder, whose last fully-connected layer (after global average pool- ing) has a fixed-dimensional output (128-D [52]). This out- put vector is normalized by its L2-norm [52]. This is the representation of the query or key. The temperature τ in Eqn.(1) is set as 0.07 [52]. The data augmentation setting follows [52]: a 224×224-pixel crop is taken from a randomly resized image, and then undergoes random color jit- tering, random horizontal flip, and random grayscale con- version, all available in PyTorch's torchvision package. Shuffling BN. Our encoders fq and fk both have Batch Normalization (BN) [33] as in the standard ResNet [28]. In experiments, we found that using BN prevents the model from learning good representations, as similarly reported in [30] (which avoids using BN). The model appears to "cheat" the pretext task and easily finds a low-loss solu- tion. This is possibly because the intra-batch communica- tion among samples (caused by BN) leaks information. We resolve this problem by shuffling BN. We train with multiple GPUs and perform BN on the samples independently for each GPU (as done in common practice). For the key encoder fk, we shuffle the sample order in the current mini-batch before distributing it among GPUs (and shuffle back after encoding); the sample order of the mini-batch for the query encoder fq is not altered. This ensures the batch statistics used to compute a query and its positive key come from two different subsets. This effectively tackles the cheating issue and allows training to benefit from BN. We use shuffled BN in both our method and its end-to- end ablation counterpart (Figure 2a). It is irrelevant to the memory bank counterpart (Figure 2b), which does not suf- fer from this issue because the positive keys are from differ- ent mini-batches in the past.

4 Experiments

We study unsupervised training performed in: ImageNet-1M (IN-1M): This is the ImageNet [**?**] train- ing set that has ~1.28 million images in 1000 classes (often called ImageNet-1K; we count the image number instead, as classes are not exploited by unsupervised learning). This dataset is well-balanced in its class distribution, and its im- ages generally contain iconic view of objects. Instagram-1B (IG-1B): Following [39], this is a dataset of ~1 billion (940M) public images from Instagram. The images are from ~1500 hashtags [39] that are related to the ImageNet categories. This dataset is relatively uncurated comparing to IN-1M, and has a long-tailed, unbalanced distribution of real-world data. This dataset contains both iconic objects and scene-level images. Training. We use SGD as our optimizer. The SGD weight decay is 0.0001 and the SGD momentum is 0.9. For IN-1M, we use a mini-batch size of 256 (N in Algorithm 1) in 8 GPUs, and an initial learning rate of 0.03. We train for 200 epochs with the learning rate multiplied by 0.1 at 120 and 160 epochs [52], taking ~53 hours training ResNet-50. For IG-1B, we use a mini-batch size of 1024 in 64 GPUs, and a learning rate of 0.12 which is exponentially decayed by 0.9× after every 62.5k iterations (64M images). We train for 1.25M iterations (~1.4 epochs of IG-1B), taking ~6 days for ResNet-50.

4.1 Linear Classification Protocol

We first verify our method by linear classification on frozen features, following a common protocol. In this sub- section we perform unsupervised pre-training on IN-1M. Then we freeze the features and train a supervised linear classifier (a fully-connected layer followed by softmax). We train this classifier on the global average pooling features of a ResNet, for 100 epochs. We report 1-crop, top-1 classifi- cation accuracy on the ImageNet validation set. For this classifier, we perform a grid search and find the optimal initial learning rate is 30 and weight decay is 0 (similarly reported in [48]). These hyper-parameters per- form consistently well for all ablation entries presented in this subsection. These hyper-parameter values imply that the feature distributions (e.g., magnitudes) can be substan- tially different from those of ImageNet supervised training, an issue we will revisit in Sec. 4.2. Ablation: contrastive loss mecha- nisms. We compare the three mechanisms that are illustrated in Figure 2. To focus on the effect of contrastive loss mechanisms, we implement all of them in the same pretext task as described in Sec. 3.3. We also use the same form of InfoNCE as the contrastive loss function, Eqn.(1). As such, the comparison is solely on the three mechanisms. The results are in Figure 3. Overall, all three mecha- nisms benefit from a larger K. A similar trend has been observed in [52, 48] under the memory bank mechanism, while here we show that this trend is more general and can be seen in all mechanisms. These results support our moti- vation of building a large dictionary. The end-to-end mechanism performs similarly to MoCo when K is small. However, the dictionary size is limited by the mini-batch size due to the end-to-end requirement. Here the largest mini-batch a high-end machine (8 Volta 32GB GPUs) can afford is 1024. More essentially, large mini-batch training is an open problem [20]: we found it necessary to use the linear learning rate scaling rule [20] here, without which the accuracy drops (by ∼21024 mini-batch). But optimizing with a larger mini-batch is harder [20], and it is questionable whether the trend can be extrapolated into a larger K even if memory is sufficient.

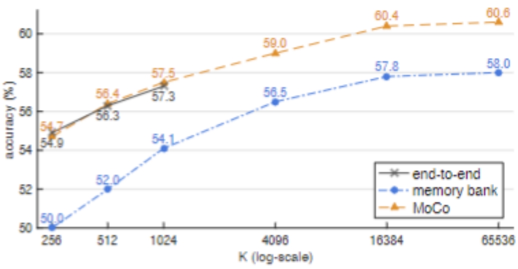

Figure 3: Comparison of three contrastive loss mechanisms un- der the ImageNet linear classification protocol. We adopt the same pretext task (Sec. 3.3) and only vary the contrastive loss mecha- nism (Figure 2). The number of negatives is K in memory bank and MoCo, and is K–1 in end-to-end (offset by one because the positive key is in the same mini-batch). The network is ResNet-50.

The memory bank [52] mechanism can support a larger dictionary size. But it is 2.6inline with our hypothesis: the keys in the memory bank are from very different encoders all over the past epoch and they are not consistent. Note the memory bank result of 58.0Ablation: momentum. The table below shows ResNet-50 accuracy with different MoCo momentum values (m in Eqn.(2)) used in pre-training (K = 4096 here) :

momentum m	0 0.9 0.99 0.999 0.9999
accuracy (%)	fail 55.2 57.8 59.0 5809

It performs reasonably well when m is in 0.99 ∼ 0.9999, showing that a slowly progressing (i.e., relatively large momentum) key encoder is beneficial. When m is too small (e.g., 0.9), the accuracy drops considerably; at the extreme of no momentum (m is 0), the training loss oscillates and fails to converge. These results support our motivation of building a consistent dictionary. Comparison with previous results. Previous unsuper- vised learning methods can differ substantially in model sizes. For a fair and comprehensive comparison, we report accuracy vs. #parameters3 trade-offs. Besides ResNet-50 (R50) [28], we also report its variants that are 2× and 4× wider (more channels), following [**?**].4 We set K = 65536 and m = 0.999. Table 1 is the comparison. MoCo with R50 performs competitively and achieves 60.6model sizes (∼24M). MoCo benefits from larger models and achieves 68.6Notably, we achieve competitive results using a standard ResNet-50 and require no specific architecture designs, e.g.,

patchified inputs [49, 30], carefully tailored receptive fields [1], or combining two networks [48]. By using an architecture that is not customized for the pretext task, it is easier to transfer features to a variety of visual tasks and make comparisons, studied in the next subsection. This paper's focus is on a mechanism for general con- trastive learning; we do not explore orthogonal factors (such as specific pretext tasks) that may further improve accuracy. As an example, "MoCo v2" [6], an extension of a prelim- inary version of this manuscript, achieves 71.1with R50 (up from 60.6augmentation and output projection head [5]. We believe that this additional result shows the generality and robust- ness of the MoCo framework.

4.2 Transferring Features

A main goal of unsupervised learning is to learn features that are transferrable. ImageNet supervised pre-training is most influential when serving as the initialization for fine- tuning in downstream tasks (e.g., [16, 15, 38, 45]). Next we compare MoCo with ImageNet supervised pre-training, transferred to various tasks including PASCAL VOC [14], COCO [37], etc. As prerequisites, we discuss two important issues involved [26]: normalization and schedules. Normalization. As noted in Sec. 4.1, features produced by unsupervised pre-training can have different distributions compared with ImageNet supervised pre-training. But a system for a downstream task often has hyper-parameters (e.g., learning rates) selected for supervised pre-training. To relieve this problem, we adopt feature normalization during fine-tuning: we fine-tune with BN that is trained (and syn- chronized across GPUs [42]), instead of freezing it by an affine layer [28]. We also use BN in the newly initialized layers (e.g., FPN [36]), which helps calibrate magnitudes. We perform normalization when fine-tuning supervised and unsupervised pre-training models. MoCo uses the same hyper-parameters as the ImageNet supervised counterpart. Schedules. If the fine-tuning schedule is long enough, training detectors from random initialization can be strong baselines, and can match the ImageNet supervised counter- part on COCO [26]. Our goal is to investigate transferabil-ity

of features, so our experiments are on controlled sched- ules, e.g., the 1× (∼12 epochs) or 2× schedules [17] for COCO, in contrast to 6×∼9× in [26]. On smaller datasets like VOC,

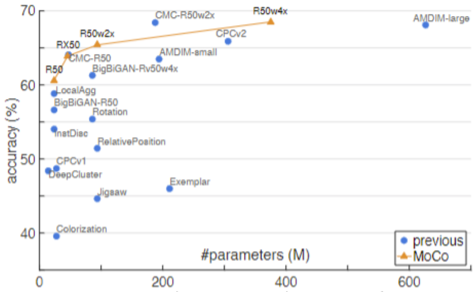

method	architecture	#params (M)	accuracy (%)
Exemplar [17]	R50w3×	211	46.0 [38]
RelativePosition [13]	R50w2×	94	51.4 [38]
Jigsaw [45]	R50w2×	94	44.6 [38]
Rotation [19]	Rv50w4×	86	55.4 [38]
Colorization [64]	R101*	28	39.6 [14]
DeepCluster [3]	VGG [53]	15	48.4 [4]
BigBiGAN [16]	R50	24	56.6
	Rv50w4×	86	61.3
methods based on contrastive learning follow:			
InstDisc [61]	R50	24	54.0
LocalAgg [66]	R50	24	58.8
CPC v1 [46]	R101*	28	48.7
CPC v2 [35]	$\text{R170}^*_{\text{wider}}$	303	65.9
CMC [56]	$\text{R50}_{\text{L+ab}}$	47	64.1†
	$\text{R50w2}\times_{\text{L+ab}}$	188	68.4†
AMDIM [2]	$\text{AMDIM}_{\text{small}}$	194	63.5†
	$\text{AMDIM}_{\text{large}}$	626	68.1†
MoCo	R50	24	60.6
	RX50	46	63.9
	R50w2×	94	65.4
	R50w4×	375	**68.6**

Table 1. **Comparison under the linear classification protocol on ImageNet**. The figure visualizes the table. All are reported as unsupervised pre-training on the ImageNet-1M training set, followed by supervised linear classification trained on frozen features, evaluated on the validation set. The parameter counts are those of the feature extractors. We compare with improved re-implementations if available (referenced after the numbers).
Notations: R101*/R170* is ResNet-101/170 with the last residual stage removed [14, 46, 35], and R170 is made wider [35]; Rv50 is a reversible net [23], RX50 is ResNeXt-50-32×8d [62].
†: *Pre-training uses FastAutoAugment [40] that is supervised by ImageNet labels.*

Figure 4: Comparison under the linear classification protocol on ImageNet. The figure visualizes the table. All are reported as unsupervised pre-training on the ImageNet-1M training set, fol- lowed by supervised linear classification trained on frozen fea- tures, evaluated on the validation set. The parameter counts are those of the feature extractors. We compare with improved re- implementations if available (referenced after the numbers). Notations: R101∗/R170∗ is ResNet-101/170 with the last residual stage removed [12, 49, 30], and R170 is made wider [30]; Rv50 is a reversible net [18], RX50 is ResNeXt-50-32×8d [53]. †: Pre-training uses FastAutoAugment [35] that is supervised by ImageNet labels.

pre-train	AP_{50}	AP	AP_{75}
random init.	64.4	37.9	38.6
super. IN-1M	81.4	54.0	59.1
MoCo IN-1M	81.1 (−0.3)	54.6 (+0.6)	59.9 (+0.8)
MoCo IG-1B	81.6 (+0.2)	55.5 (+1.5)	61.2 (+2.1)

(a) Faster R-CNN, R50-dilated-C5

pre-train	AP_{50}	AP	AP_{75}
random init.	60.2	33.8	33.1
super. IN-1M	81.3	53.5	58.8
MoCo IN-1M	81.5 (+0.2)	55.9 (+2.4)	62.6 (+3.8)
MoCo IG-1B	82.2 (+0.9)	57.2 (+3.7)	63.7 (+4.9)

(b) Faster R-CNN, R50-C4

Table 2. **Object detection fine-tuned on PASCAL VOC** `trainval07+12`. Evaluation is on `test2007`: AP_{50} (default VOC metric), AP (COCO-style), and AP_{75}, averaged over 5 trials. All are fine-tuned for 24k iterations (~23 epochs). In the brackets are the gaps to the ImageNet supervised pre-training counterpart. In green are the gaps of at least +0.5 point.

Figure 5: Object detection fine-tuned on PASCAL VOC trainval07+12. Evaluation is on test2007: AP50 (default VOC metric), AP (COCO-style), and AP75, averaged over 5 trials. All are fine-tuned for 24k iterations (∼23 epochs). In the brackets are the gaps to the ImageNet supervised pre-training counterpart. In green are the gaps of at least +0.5 point.

	R50-dilated-C5			R50-C4		
pre-train	AP_{50}	AP	AP_{75}	AP_{50}	AP	AP_{75}
end-to-end	79.2	52.0	56.6	80.4	54.6	60.3
memory bank	79.8	52.9	57.9	80.6	54.9	60.6
MoCo	**81.1**	**54.6**	**59.9**	**81.5**	**55.9**	**62.6**

Table 3. **Comparison of three contrastive loss mechanisms** on PASCAL VOC object detection, fine-tuned on `trainval07+12` and evaluated on `test2007` (averages over 5 trials). All models are implemented by us (Figure 3), pre-trained on IN-1M, and fine-tuned using the same settings as in Table 2.

Figure 6: Comparison of three contrastive loss mechanisms on PASCAL VOC object detection, fine-tuned on trainval07+12 and evaluated on test2007 (averages over 5 trials). All models are implemented by us (Figure 3), pre-trained on IN-1M, and fine- tuned using the same settings as in Table 2.

pre-train	AP_{50} RelPos, by [14]	Multi-task [14]	Jigsaw, by [26]	LocalAgg [66]	MoCo	AP MoCo	AP_{75} Multi-task [14]	MoCo
super. IN-1M	74.2	74.2	70.5	74.6	74.4	42.4	44.3	42.7
unsup. IN-1M	66.8 (−7.4)	70.5 (−3.7)	61.4 (−9.1)	69.1 (−5.5)	74.9 (+0.5)	46.6 (+4.2)	43.9 (−0.4)	50.1 (+7.4)
unsup. IN-14M	-	-	69.2 (−1.3)	-	75.2 (+0.8)	46.9 (+4.5)	-	50.2 (+7.5)
unsup. YFCC-100M	-	-	66.6 (−3.9)	-	74.7 (+0.3)	45.9 (+3.5)	-	49.0 (+6.3)
unsup. IG-1B	-	-	-	-	75.6 (+1.2)	47.6 (+5.2)	-	51.7 (+9.0)

Table 4. **Comparison with previous methods on object detection fine-tuned on PASCAL VOC** `trainval2007`. Evaluation is on `test2007`. The ImageNet supervised counterparts are from the respective papers, and are reported as having *the same structure* as the respective unsupervised pre-training counterparts. All entries are based on the C4 backbone. The models in [14] are R101 v2 [34], and others are R50. The RelPos (relative position) [13] result is the best single-task case in the Multi-task paper [14]. The Jigsaw [45] result is from the ResNet-based implementation in [26]. Our results are with 9k-iteration fine-tuning, averaged over 5 trials. In the brackets are the gaps to the ImageNet supervised pre-training counterpart. In green are the gaps of at least +0.5 point.

Figure 7: Comparison with previous methods on object detection fine-tuned on PASCAL VOC trainval2007. Evaluation is on test2007. The ImageNet supervised counterparts are from the respective papers, and are reported as having the same structure as the respective unsupervised pre-training counterparts. All entries are based on the C4 backbone. The models in [12] are R101 v2 [29], and others are R50. The RelPos (relative position) [11] result is the best single-task case in the Multi-task paper [12]. The Jigsaw [40] result is from the ResNet-based implementation in [21]. Our results are with 9k-iteration fine-tuning, averaged over 5 trials. In the brackets are the gaps to the ImageNet supervised pre-training counterpart. In green are the gaps of at least +0.5 point.

training longer may not catch up [26]. Nonetheless, in our fine-tuning, MoCo uses the same schedule as the ImageNet supervised counterpart, and ran- dom initialization results are provided as references. Put together, our fine-tuning uses the same setting as the supervised pre-training counterpart. This may place MoCo at a disadvantage. Even so, MoCo is competitive. Doing so also makes it feasible to present comparisons on multiple datasets/tasks, without extra hyper-parameter search.

4.2.1 PASCAL VOC Object Detection

Setup. The detector is Faster R-CNN [45] with a backbone of R50-dilated-C5 or R50-C4 [27] (details in appendix), with BN tuned, implemented in [51]. We fine-tune all lay- ers end-to-end. The image scale is [480, 800] pixels during training and 800 at inference. The same setup is used for all entries, including the supervised pre-training baseline. We evaluate the default VOC metric of AP50 (i.e., IoU threshold is 50and AP75. Evaluation is on the VOC test2007 set. Ablation: backbones. Table 2 shows the results fine-tuned on trainval07+12 (∼16.5k images). For R50-dilated- C5 (Table 2a), MoCo pre-trained on IN-1M is comparable to the supervised pre-training counterpart, and MoCo pre- trained on IG-1B surpasses it. For R50-C4 (Table 2b), MoCo with IN-1M or IG-1B is better than the supervised counterpart: up to +0.9 AP50, +3.7 AP, and +4.9 AP75. Interestingly, the transferring accuracy depends on the detector structure. For the C4 backbone, by default used in existing ResNet-based results [12, 52, 21, 56], the ad- vantage of unsupervised pre-training is larger. The relation between pre-training vs. detector structures has been veiled in the past, and should be a factor under consideration. Ablation: contrastive loss mechanisms. We point out that these results are partially because we establish solid detec- tion baselines for contrastive learning. To pin-point the gain that is solely contributed by using the MoCo mechanism in contrastive learning, we fine-tune the models pre-trained with the end-to-end or memory bank mechanism, both im- plemented by us (i.e., the best ones in Figure 3), using the same fine-tuning setting as MoCo. These competitors perform decently (Table 3). Their AP and AP75 with the C4 backbone are also higher than the ImageNet supervised counterpart's, c.f . Table 2b, but other metrics are lower. They are worse than MoCo in all metrics. This shows the benefits of MoCo. In addition, how to train these competitors in larger-scale data is an open question, and they may not benefit from IG-1B. Comparison with previous results. Following the com- petitors, we fine-tune on trainval2007 (∼5k images) using the C4 backbone. The comparison is in Table 4. For the AP50 metric, no previous method can catch up with its respective supervised pre-training counterpart. MoCo pre-trained on any of IN-1M, IN-14M (full Ima- geNet), YFCC-100M [47], and IG-1B can outperform the supervised baseline. Large gains are seen in the more strin- gent metrics: up to +5.2 AP and +9.0 AP75. These gains are larger than the gains seen in trainval07+12 (Table 2b).

4.2.2 COCO Object Detection and Segmentation

Setup. The model is Mask R-CNN [27] with the FPN [36] or C4 backbone, with BN tuned, implemented in [51]. The image scale is in [640, 800] pixels during training and is 800 at inference. We fine-tune all layers end-to-end. We fine- tune on the train2017 set (∼118k images) and evaluate on val2017. The schedule is the default 1× or 2× in [17]. Results. Table 5 shows the results on COCO with the FPN (Table 5a, b) and C4 (Table 5c, d) backbones. With the 1× schedule, all models (including the ImageNet super- vised counterparts) are heavily under-trained, as indicated by the ∼2 points gaps to the 2× schedule cases. With the 2× schedule, MoCo is better than its ImageNet supervised counterpart in all metrics in both backbones.

4.2.3 More Downstream Tasks

Table 6 shows more downstream tasks (implementation details in appendix). Overall, MoCo performs competitively

with ImageNet supervised pre-training: COCO keypoint detection: supervised pre-training has no clear advantage over random initialization, whereas MoCo outperforms in all metrics. COCO dense pose estimation [22]: MoCo substantially outperforms supervised pre-training, e.g., by 3.7 points in APdp 75, in this highly localization-sensitive task. LVIS v0.5 instance segmentation [23]: this task has ∼1000 long-tailed distributed categories. Specifically in LVIS for the Ima- geNet supervised baseline, we find fine- tuning with frozen BN (24.4 APmk) is better than tunable BN (details in appendix). So we compare MoCo with the better supervised pre-training variant in this task. MoCo with IG-1B surpasses it in all metrics. Cityscapes instance segmentation [8]: MoCo with IG-1B is on

pre-train	AP^{bb}	AP^{bb}_{50}	AP^{bb}_{75}	AP^{mk}	AP^{mk}_{50}	AP^{mk}_{75}
random init.	31.0	49.5	33.2	28.5	46.8	30.4
super. IN-1M	38.9	59.6	42.7	35.4	56.5	38.1
MoCo IN-1M	38.5 (−0.4)	58.9 (−0.7)	42.0 (−0.7)	35.1 (−0.3)	55.9 (−0.6)	37.7 (−0.4)
MoCo IG-1B	38.9 (0.0)	59.4 (−0.2)	42.3 (−0.4)	35.4 (0.0)	56.5 (0.0)	37.9 (−0.2)

(a) Mask R-CNN, R50-**FPN**, **1**× schedule

pre-train	AP^{bb}	AP^{bb}_{50}	AP^{bb}_{75}	AP^{mk}	AP^{mk}_{50}	AP^{mk}_{75}
random init.	36.7	56.7	40.0	33.7	53.8	35.9
super. IN-1M	40.6	61.3	44.4	36.8	58.1	39.5
MoCo IN-1M	40.8 (+0.2)	61.6 (+0.3)	44.7 (+0.3)	36.9 (+0.1)	58.4 (+0.3)	39.7 (+0.2)
MoCo IG-1B	41.1 (+0.5)	61.8 (+0.5)	45.1 (+0.7)	37.4 (+0.6)	59.1 (+1.0)	40.2 (+0.7)

(b) Mask R-CNN, R50-**FPN**, **2**× schedule

pre-train	AP^{bb}	AP^{bb}_{50}	AP^{bb}_{75}	AP^{mk}	AP^{mk}_{50}	AP^{mk}_{75}
random init.	26.4	44.0	27.8	29.3	46.9	30.8
super. IN-1M	38.2	58.2	41.2	33.3	54.7	35.2
MoCo IN-1M	38.5 (+0.3)	58.3 (+0.1)	41.6 (+0.4)	33.6 (+0.3)	54.8 (+0.1)	35.6 (+0.4)
MoCo IG-1B	39.1 (+0.9)	58.7 (+0.5)	42.2 (+1.0)	34.1 (+0.8)	55.4 (+0.7)	36.4 (+1.2)

(c) Mask R-CNN, R50-**C4**, **1**× schedule

pre-train	AP^{bb}	AP^{bb}_{50}	AP^{bb}_{75}	AP^{mk}	AP^{mk}_{50}	AP^{mk}_{75}
random init.	35.6	54.6	38.2	31.4	51.5	33.5
super. IN-1M	40.0	59.9	43.1	34.7	56.5	36.9
MoCo IN-1M	40.7 (+0.7)	60.5 (+0.6)	44.1 (+1.0)	35.4 (+0.7)	57.3 (+0.8)	37.6 (+0.7)
MoCo IG-1B	41.1 (+1.1)	60.7 (+0.8)	44.8 (+1.7)	35.6 (+0.9)	57.4 (+0.9)	38.1 (+1.2)

(d) Mask R-CNN, R50-**C4**, **2**× schedule

Table 5. **Object detection and instance segmentation fine-tuned on COCO**: bounding-box AP (AP^{bb}) and mask AP (AP^{mk}) evaluated on `val2017`. In the brackets are the gaps to the ImageNet supervised pre-training counterpart. In green are the gaps of at least +0.5 point.

Figure 8: Object detection and instance segmentation fine-tuned on COCO: bounding-box AP (APbb) and mask AP (APmk) evaluated on val2017. In the brackets are the gaps to the ImageNet supervised pre-training counterpart. In green are the gaps of at least +0.5 point.

pre-train	COCO keypoint detection AP^{kp}	AP^{kp}_{50}	AP^{kp}_{75}
random init.	65.9	86.5	71.7
super. IN-1M	65.8	86.9	71.9
MoCo IN-1M	66.8 (+1.0)	87.4 (+0.5)	72.5 (+0.6)
MoCo IG-1B	66.9 (+1.1)	87.8 (+0.9)	73.0 (+1.1)

pre-train	COCO dense pose estimation AP^{dp}	AP^{dp}_{50}	AP^{dp}_{75}
random init.	39.4	78.5	35.1
super. IN-1M	48.3	85.6	50.6
MoCo IN-1M	50.1 (+1.8)	86.8 (+1.2)	53.9 (+3.3)
MoCo IG-1B	50.6 (+2.3)	87.0 (+1.4)	54.3 (+3.7)

pre-train	LVIS v0.5 instance segmentation AP^{mk}	AP^{mk}_{50}	AP^{mk}_{75}
random init.	22.5	34.8	23.8
super. IN-1M†	24.4	37.8	25.8
MoCo IN-1M	24.1 (−0.3)	37.4 (−0.4)	25.5 (−0.3)
MoCo IG-1B	24.9 (+0.5)	38.2 (+0.4)	26.4 (+0.6)

pre-train	Cityscapes instance seg. AP^{mk}	AP^{mk}_{50}	Semantic seg. (mIoU) Cityscapes	VOC
random init.	25.4	51.1	65.3	39.5
super. IN-1M	32.9	59.6	74.6	74.4
MoCo IN-1M	32.3 (−0.6)	59.3 (−0.3)	75.3 (+0.7)	72.5 (−1.9)
MoCo IG-1B	32.9 (0.0)	60.3 (+0.7)	75.5 (+0.9)	73.6 (−0.8)

Table 6. **MoCo *vs*. ImageNet supervised pre-training, fine-tuned on various tasks**. For each task, the same architecture and schedule are used for all entries (see appendix). In the brackets are the gaps to the ImageNet supervised pre-training counterpart. In green are the gaps of at least +0.5 point.

†: this entry is with BN frozen, which improves results; see main text.

Figure 9: MoCo vs. ImageNet supervised pre-training, fine-tuned on various tasks. For each task, the same architecture and schedule are used for all entries (see appendix). In the brackets are the gaps to the ImageNet supervised pre-training counterpart. In green are the gaps of at least +0.5 point. †: this entry is with BN frozen, which improves results; see main text.

par with its supervised pre-training counterpart in APmk, and is higher in APmk 50 . Semantic segmentation: On Cityscapes [8], MoCo out- performs its supervised pre-training counterpart by up to 0.9 point. But on VOC semantic segmentation, MoCo is worse by at least 0.8 point, a negative case we have observed. Summary. In sum, MoCo can outperform its ImageNet supervised pre-training counterpart in 7 detection or seg- mentation tasks.5 Besides, MoCo is on par on Cityscapes instance segmentation, and lags behind on VOC semantic segmentation; we show another comparable case on iNatu- ralist [32] in appendix. Overall, MoCo has largely closed the gap between unsupervised and supervised representa- tion learning in multiple vision tasks. Remarkably, in all these tasks, MoCo pre-trained on IG-1B is consistently better than MoCo pre-trained on IN-1M. This shows that MoCo can perform well on this large-scale, relatively uncurated dataset. This represents a scenario towards real-world unsupervised learning.

5 Discussion and Conclusion

Our method has shown positive results of unsupervised learning in a variety of computer vision tasks and datasets. A few open questions are worth discussing. MoCo's im- provement from IN-1M to IG-1B is consistently noticeable but relatively small, suggesting that the larger-scale data may not be fully exploited. We hope an advanced pretext task will improve this. Beyond the simple instance discrim- ination task [52], it is possible to adopt MoCo for pretext tasks like masked auto-encoding, e.g., in language [10] and in vision [49]. We hope MoCo will be useful with other pretext tasks that involve contrastive learning.

References

[1] Philip Bachman, R Devon Hjelm, and William Buchwalter. Learning representations by maximizing mutual information across views. *arXiv:1906.00910*, 2019.

[2] Mathilde Caron, Piotr Bojanowski, Armand Joulin, and Matthijs Douze. Deep clustering for unsupervised learning of visual features. In *ECCV*, 2018.

[3] Mathilde Caron, Piotr Bojanowski, Julien Mairal, and Armand Joulin. Unsupervised pre-training of image features on non-curated data. In *ICCV*, 2019.

[4] Ken Chatfield, Victor Lempitsky, Andrea Vedaldi, and Andrew Zisserman. The devil is in the details: an evaluation of recent feature encoding methods. In *BMVC*, 2011.

[5] Ting Chen, Simon Kornblith, Mohammad Norouzi, and

Geoffrey Hinton. A simple framework for contrastive learning of visual representations. *arXiv:2002.05709*, 2020.

[6] Xinlei Chen, Haoqi Fan, Ross Girshick, and Kaiming He. Improved baselines with momentum contrastive learning. *arXiv:2003.04297*, 2020.

[7] Adam Coates and Andrew Ng. The importance of encoding versus training with sparse coding and vector quantization. In *ICML*, 2011.

[8] Marius Cordts, Mohamed Omran, Sebastian Ramos, Timo Rehfeld, Markus Enzweiler, Rodrigo Benenson, Uwe Franke, Stefan Roth, and Bernt Schiele. The cityscapes dataset for semantic urban scene understanding. In *CVPR*, 2016.

[9] Jia Deng, Wei Dong, Richard Socher, Li-Jia Li, Kai Li, and Li Fei-Fei. Imagenet: A large-scale hierarchical image database. In *CVPR*, 2019.

[10] Jacob Devlin, Ming-Wei Chang, Kenton Lee, and Kristina Toutanova. Bert: Pre-training of deep bidirectional transformers for language understanding. In *NAACL*, 2019.

[11] Carl Doersch, Abhinav Gupta, and Alexei A Efros. Unsupervised visual representation learning by context prediction. In *ICCV*, 2015.

[12] Carl Doersch and Andrew Zisserman. Multi-task self-supervised visual learning. In *ICCV*, 2017.

[13] Alexey Dosovitskiy, Jost Tobias Springenberg, Martin Riedmiller, and Thomas Brox. Discriminative unsupervised feature learning with convolutional neural networks. In *NeurIPS*, 2014.

[14] Mark Everingham, Luc Van Gool, Christopher KI Williams, John Winn, and Andrew Zisserman. The pascal visual object classes (voc) challenge. *IJCV*, 2010.

[15] Ross Girshick. Fast r-cnn. In *ICCV*, 2015.

[16] Ross Girshick, Jeff Donahue, Trevor Darrell, and Jitendra Malik. Rich feature hierarchies for accurate object detection and semantic segmentation. In *CVPR*, 2014.

[17] Ross Girshick, Ilija Radosavovic, Georgia Gkioxari, Piotr Dollár, and Kaiming He. Detectron. 2018.

[18] Aidan N Gomez, Mengye Ren, Raquel Urtasun, and Roger B Grosse. The reversible residual network: Backpropagation without storing activations. In *NeurIPS*, 2017.

[19] Ian Goodfellow, Jean Pouget-Abadie, Mehdi Mirza, Bing Xu, David Warde-Farley, Sherjil Ozair, Aaron Courville, and Yoshua Bengio. Generative adversarial nets. In *NeurIPS*, 2014.

[20] Priya Goyal, Piotr Dollár, Ross Girshick, Pieter Noordhuis, Lukasz Wesolowski, Aapo Kyrola, Andrew Tulloch, Yangqing Jia, and Kaiming He. Accurate, large minibatch sgd: Training imagenet in 1 hour. *arXiv:1706.02677*, 2017.

[21] Priya Goyal, Dhruv Mahajan, Abhinav Gupta, and Ishan Misra. Scaling and benchmarking self-supervised visual representation learning. In *ICCV*, 2019.

[22] Rıza Alp Güler, Natalia Neverova, and Iasonas Kokkinos. Densepose: Dense human pose estimation in the wild. In *CVPR*, 2018.

[23] Agrim Gupta, Piotr Dollar, and Ross Girshick. Lvis: A dataset for large vocabulary instance segmentation. In *CVPR*, 2019.

[24] Michael Gutmann and Aapo Hyvärinen. Noise-contrastive estimation: A new estimation principle for unnormalized statistical models. In *AISTATS*, 2010.

[25] Raia Hadsell, Sumit Chopra, and Yann LeCun. Dimensionality reduction by learning an invariant mapping. In *CVPR*, 2016.

[26] Kaiming He, Ross Girshick, and Piotr Dollár. Rethinking imagenet pre-training. In *ICCV*, 2019.

[27] Kaiming He, Georgia Gkioxari, Piotr Dollár, and Ross Girshick. Mask r-cnn. In *ICCV*, 2017.

[28] Kaiming He, Xiangyu Zhang, Shaoqing Ren, and Jian Sun. Deep residual learning for image recognition. In *CVPR*, 2016.

[29] Kaiming He, Xiangyu Zhang, Shaoqing Ren, and Jian Sun. Identity mappings in deep residual networks. In *ECCV*, 2016.

[30] Olivier J Hénaff, Ali Razavi, Carl Doersch, SM Eslami, and Aaron van den Oord. Data-efficient image recognition with contrastive predictive coding. *arXiv:1905.09272*, 2019.

[31] R Devon Hjelm, Alex Fedorov, Samuel Lavoie-Marchildon, Karan Grewal, Adam Trischler, and Yoshua Bengio. Learning deep representations by mutual information estimation and maximization. In *ICLR*, 2019.

[32] Grant Van Horn, Oisin Mac Aodha, Yang Song, Yin Cui, Chen Sun, Alex Shepard, Hartwig Adam, Pietro Perona, and Serge Belongie. The inaturalist species classification and detection dataset. In *CVPR*, 2018.

[33] Sergey Ioffe and Christian Szegedy. Batch normalization: Accelerating deep network training by reducing internal covariate shift. In *ICML*, 2015.

[34] Yann LeCun, Bernhard Boser, John S Denker, Donnie Henderson, Richard E Howard, Wayne Hubbard, and Lawrence D Jackel. Backpropagation applied to handwritten zip code recognition. *Neural computation*, 1989.

[35] Sungbin Lim, Ildoo Kim, Taesup Kim, Chiheon Kim, and Sungwoong Kim. Fast autoaugment. *arXiv:1905.00397*, 2019.

[36] Tsung-Yi Lin, Piotr Dollár, Ross Girshick, Kaiming He, Bharath Hariharan, and Serge Belongie. Feature pyramid networks for object detection. In *CVPR*, 2017.

[37] Tsung-Yi Lin, Michael Maire, Serge Belongie, James Hays, Pietro Perona, Deva Ramanan, Piotr Dollár, and C Lawrence Zitnick. Microsoft coco: Common objects in context. In *ECCV*, 2014.

[38] Jonathan Long, Evan Shelhamer, and Trevor Darrell. Fully convolutional networks for semantic segmentation. In *CVPR*, 2015.

[39] Dhruv Mahajan, Ross Girshick, Vignesh Ramanathan, Kaiming He, Manohar Paluri, Yixuan Li, Ashwin Bharambe, and Laurens van der Maaten. Exploring the limits of weakly supervised pretraining. In *ECCV*, 2018.

[40] Mehdi Noroozi and Paolo Favaro. Unsupervised learning of visual representations by solving jigsaw puzzles. In *ECCV*, 2016.

[41] Deepak Pathak, Philipp Krahenbuhl, Jeff Donahue, Trevor Darrell, and Alexei A Efros. Context encoders: Feature learning by inpainting. In *CVPR*, 2016.

[42] Chao Peng, Tete Xiao, Zeming Li, Yuning Jiang, Xiangyu Zhang, Kai Jia, Gang Yu, and Jian Sun. Megdet: A large mini-batch object detector. In *CVPR*, 2018.

[43] Alec Radford, Karthik Narasimhan, Tim Salimans, and Ilya Sutskever. Improving language understanding by generative pre-training. 2018.

[44] Alec Radford, Jeffrey Wu, Rewon Child, David Luan, Dario Amodei, and Ilya Sutskever. Language models are unsupervised multitask learners. 2019.

[45] Saoqing Ren, Kaiming He, Ross Girshick, and Jian Sun. Faster r-cnn: Towards real-time object detection with region proposal networks. In *NeurIPS*, 2015.

[46] Jost Sivic and Andrew Zisserman. Video google: a text retrieval approach to object matching in videos. In *ICCV*, 2003.

[47] Bart Thomee, David A Shamma, Gerald Friedland, Benjamin Elizalde, Karl Ni, Douglas Poland, Damian Borth, and Li-Jia Li. Yfcc100m: The new data in multimedia research. *Communications of the ACM*, 2016.

[48] Yonglong Tian, Dilip Krishnan, and Phillip Isola. Contrastive multiview coding. *arXiv:1906.05849*, 2019.

[49] Aaron van den Oord, Yazhe Li, and Oriol Vinyals. Representation learning with contrastive predictive coding. *arXiv:1807.03748*, 2018.

[50] Xiaolong Wang and Abhinav Gupta. Unsupervised learning of visual representations using videos. In *ICCV*, 2015.

[51] Yuxin Wu, Alexander Kirillov, Francisco Massa, Wan-Yen Lo, and Ross Girshick. Detectron2, 2019.

[52] Zhirong Wu, Yuanjun Xiong, Stella Yu, and Dahua Lin. Unsupervised feature learning via non-parametric instance discrimination. In *CVPR*, 2018. Updated version accessed at: https://arxiv.org/abs/1805.01978v1.

[53] Saining Xie, Ross Girshick, Piotr Dollár, Zhuowen Tu, and Kaiming He. Aggregated residual transformations for deep neural networks. In *CVPR*, 2017.

[54] Mang Ye, Xu Zhang, Pong C Yuen, and Shih-Fu Chang. Unsupervised embedding learning via invariant and spreading instance feature. In *CVPR*, 2019.

[55] Richard Zhang, Phillip Isola, and Alexei A Efros. Colorful image colorization. In *ECCV*, 2016.

[56] Chengxu Zhuang, Alex Lin Zhai, and Daniel Yamins. Local aggregation for unsupervised learning of visual embeddings. In *ICCV*, 2019. Additional results accessed from supplementary materials.